

Control of the charge and the nonlinear oscillation of dust particles by alternating current voltage superposition on the cathode in a direct current discharge

S. Park

Division of Optical Metrology, Korea Research Institute of Standards and Science, 1 Doryong-dong, Yuseong-gu, Daejeon 305-340, Korea

C. R. Seon and W. Choe^{a)}

Department of Physics, Korea Advanced Institute of Science and Technology, 373-1 Guseong-dong, Yuseong-gu, Daejeon 305-701, Korea

(Received 19 February 2005; accepted 29 April 2005; published online 9 June 2005)

Experimental and theoretical studies were conducted to investigate the control of charge and modification of nonlinear oscillations of externally injected dust particles in a dc discharge. The superposition of ac voltage on a dc cathode led to plasma density modulation, which brought about a drastic change of particle oscillation characteristics. Examples of the changes include disappearance of the subharmonic resonance peak and hysteresis as the ac superposition voltage was increased, which is attributed to the fact that the ac superposition made sheath structure less nonlinear and less parametrically resonant. In addition, as the ac frequency decreased from 5 kHz to 1 kHz at the same ac voltage (15 V), the subharmonic peak became weakened along with its frequency. This result demonstrates that the dust charge is the main parameter in determining occurrence of the subharmonic resonance peak. We consequently expect that modification of the oscillation dynamics of dust particles and furthermore the separate control of the charge may be possible by the ac modulation of the dc biased cathode. © 2005 American Institute of Physics.

[DOI: 10.1063/1.1938127]

I. INTRODUCTION

Dust particles frequently appear in industrial plasmas utilized for sputtering, deposition, etching, and so on due to reactive chemical or physical processes. The dust particles, charged by plasma electrons and ions, experience various forces such as gravity, electrostatic, and ion drag force. As a result of charging and force balancing, the dust particles are likely to be localized or trapped around the plasma-sheath boundary, which is regarded as the main scenario of plasma contamination in processing plasmas.¹ For this reason, dust particle control is one of the important research issues because it can provide a way of alleviating dust contamination problem in many plasma-aided microelectronics fabrication processes. Recent studies reported that the shape of the particle trap and the collective motion of the particles could be manipulated by a static electric or magnetic field by simply changing electrode configurations.^{2,3} The work presented here, on the other hand, aims to independently control fundamental parameters directly related to the dust particle, more specifically particle charge, while other plasma parameters remain fixed. In this study, the oscillatory motion of the dust particle trapped at the plasma-sheath boundary was examined as an indicator of the dust charge modification.

The oscillatory behavior of a levitated dust particle provides important hints for understanding the particle dynamics in plasmas. Recent studies on the externally driven particle oscillation demonstrated various nonlinear features such as

appearance of secondary resonances, hysteresis, amplitude-dependent frequency shift of the resonance peaks, and the conditions for development of the nonlinear features were investigated.^{4-6,8,7,9,10} Possible causes of the nonlinear oscillation characteristics include nonlinearity of the trapping forces, spatial dependence of the driving force and dust charge, and low neutral gas damping due to low gas pressure. In this work, controlling the dynamic behavior of dust particles, especially the nonlinear dust oscillatory motion, was attempted by changing the plasma structure at the sheath via superposing an ac voltage on the dc biased cathode. The superposition of the ac voltage with a relatively faster frequency than a typical particle oscillation frequency alters the plasma structure too fast for the dust particle to follow the changes. In this way, the particle dynamics are determined by the time-averaged plasma structure rather than the instantaneous one. Furthermore, by adjusting the ac modulation frequency, the particle charge can be controlled independently if the modulation frequency is provided in such a way that the time scale of dust charging is comparable to that of the ac modulation. This approach enables us not only to control the dynamic behavior but also to investigate the role of the dust charge in its nonlinear oscillation. The detailed description of the ac modulation is presented in Sec. III.

II. EXPERIMENTAL SETUP

Experiments were performed using a cylindrical dc plasma source shown in Fig. 1. It consisted of a cathode of 8 cm diameter placed at the bottom and a center-holed anode

^{a)}Electronic mail: wchoe@kaist.ac.kr

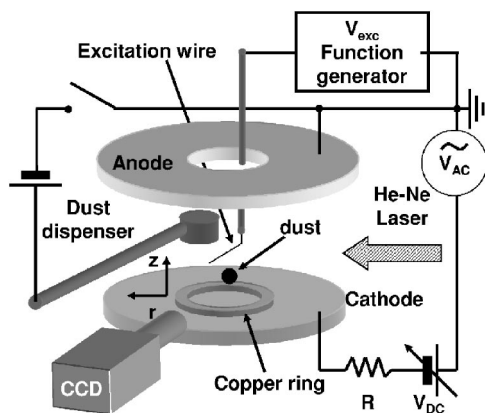


FIG. 1. Schematic diagram of the experimental setup.

(outer diameter=11 cm, inner diameter=6 cm) placed at the top. The distance between the anode and cathode was 6 cm. A discharge power supply system was prepared to enable the ac voltage superposition on the dc cathode voltage. The sinusoidal ac voltage V_{ac} ranged from 0 V to 25 V in the frequency f_{ac} range of 500 Hz–20 kHz. A dust dispenser made of a simple beep speaker was used to externally inject $1.5 \mu\text{m}$ SiO_2 or $2.0 \mu\text{m}$ melamine formaldehyde monodisperse particles inside the plasma. A patch of a fine tungsten wire of 0.2 mm diameter located at 24 mm above the cathode was used to excite the vertical oscillatory motion of the trapped and levitated particles. It was connected to a function generator to provide an oscillating voltage V_{exc} of 0–10 V in 0–150 Hz frequency. It is pointed out that this “slow” voltage source for exciting particle oscillations (V_{exc}) should not be confused with the “fast” ac voltage source for cathode modulation (V_{ac}) described above.

A typical glow discharge was produced at a typical cathode voltage of $V_C = -320$ V and current of $I_p = 1$ mA with argon gas feeding at 250 mTorr. To confine the externally injected particles around the radial center of the cathode, a copper electrode (4.8 cm outer diameter, 3.7 cm inner diameter) was placed on the cathode, with which the injected particles were trapped above the cathode surface. For instance, $1.5 \mu\text{m}$ particles were levitated about 10 mm above the cathode surface. During the experiments, dust oscillation spectra at a given amplitude V_{ac} and frequency f_{ac} superposed to the cathode were measured. The oscillation spectra were obtained for the forward and backward frequency sweeps in which V_{exc} applied to the excitation wire was varied by every 0.5 Hz. For visualization and recording of the particle oscillation trajectories, a light scattering method was implemented using a 632.8 nm He–Ne laser. The scattered light intensity was recorded using a set of zoom lens, a charge-coupled device detector, and a general video capture board. A home-made image processing software was utilized to extract the oscillation amplitude from the captured movie that contained the particle trajectories.

III. THEORY AND SIMULATION METHOD

Superposition of ac voltage on the dc cathode brings about the modulation of cathode voltage, which results in the

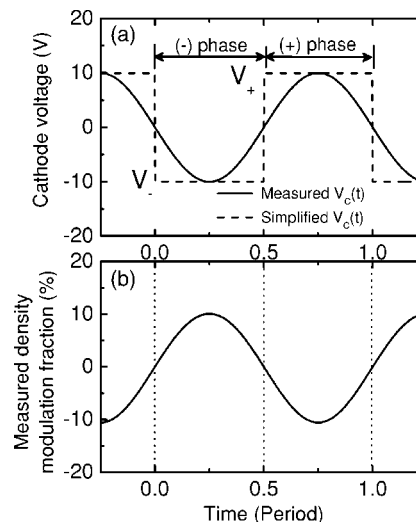


FIG. 2. (a) Cathode voltage wave form when V_C (V) = $-320 + 10 \sin(2\pi f_{ac}t)$, where “measured V_C ” indicates the measured cathode voltage. It was simplified to a square wave form (simplified V_C) for the sake of easy calculation. (b) Measured fractional density modulated by ac voltage superposed on the cathode. For example, 0% means unmodulated and 10% represents the density varied from the unmodulated density to its 10%.

modulation of bulk plasma density as shown in Fig. 2. Consequently, the bulk plasma density modulation induces the position-dependent modulation of the plasma parameters such as electron and ion density profiles, potential profile, electric field profile, etc. If the frequency of the superposing ac voltage is low enough for the trapped particles to respond, the cathode modulation will cause the dust particles to parametrically oscillate, i.e., the instantaneous motion of the particles is directly subject to the cathode modulation.^{7,8} On the other hand, under high ac frequency to which the particles cannot respond, no particle oscillation will take place. Instead, the levitated particles will experience time averaged field and plasma parameters, not instantaneous ones. Therefore, the electric field experienced by the dust particle, for instance, can be reduced to the time average of its instantaneous value. However, the dust charge should be determined in a more complex manner because the charging procedure has a finite relaxation or equilibrium time and its time scale may still be comparable to that of the cathode modulation. Actually, the time-averaged electric field felt by the dust particle has no dependence on the applied ac frequency if the frequency dependence of the plasma discharge itself is negligible, but the dust charge may vary with the ac frequency if the charging time is comparable to $1/f_{ac}$. Motivated by the idea, we studied a possibility of modifying the dust charge using the ac-modulated cathode by investigating the nonlinear oscillation characteristics of the trapped dust particles. In the remaining part of this section, the model for describing the plasma sheath and the dust oscillation under the ac modulated cathode is discussed in detail.

A. Plasma sheath, dust charge, and exerted forces

In order to properly describe dust oscillation under the ac modulation of the cathode, a sheath model and a dust oscillation model of a plasma of which density is modulated

are required. Prior to a further discussion, we assume that the plasma variation just follows the ac modulation of the cathode since $2\pi f_{ac} \ll \omega_{pe}, \omega_{pi}$, where ω_{pe} and ω_{pi} are electron and ion plasma frequencies, respectively. As depicted in Fig. 2, the ac-superposed cathode induced the modulation of the bulk plasma density which was measured in the bulk plasma by a Langmuir probe. The plasma density was proportional to the cathode voltage. For the sake of an easy calculation of the plasma structure, the sinusoidal wave form (solid line) of the modulated cathode voltage [$V_C = V_{dc} + V_{ac} \sin(2\pi f_{ac} t)$] was simplified to the square wave form (dashed line). This simplification enabled us to avoid a time-consuming calculation because one period is just divided into (+) phase and (-) phase, and the plasma structure is only calculated when the cathode voltage is $V_+ \equiv V_{dc} + V_{ac}$ and $V_- \equiv V_{dc} - V_{ac}$. For convenience, the subscripts + and - are defined to indicate whether calculations are performed at $V_C = V_+$ or $V_C = V_-$. For example, E_+ and E_- denote the electric field at (+) and (-) phases, respectively, and the time-averaged electric field \bar{E} is simply expressed as the mean value of the electric field at each phase, $(E_+ + E_-)/2$. It is pointed out that the parameters such as electric field should be time averaged over the time scale of $1/f_{ac}$ and not over the dust oscillation time scale in order to study the dynamics of the dust particles.

In the case of a small-sized dust particle, it is likely to be trapped in the presheath region. Thus, a plasma-sheath model should be capable of dealing with the presheath region as well as the sheath region.¹⁰ In order to take the gas pressure effect into account, ion-neutral collisions should also be included. With the above considerations, the plasma-sheath modeling was performed by solving a set of equations expressed as¹¹⁻¹³

$$n_{i\pm} u_{i\pm} = n_{0\pm} u_B = \text{const}, \quad (1)$$

$$n_{e\pm} = n_{0\pm} \exp\left(\frac{e\phi_{\pm}}{kT_e}\right), \quad (2)$$

$$m_i n_{i\pm} u_{i\pm} \frac{du_{i\pm}}{dz} = -n_{i\pm} e \frac{d\phi_{\pm}}{dz} - m_i n_{i\pm} \frac{\pi}{2\lambda_i} u_{i\pm}^2, \quad (3)$$

$$\epsilon_0 \frac{d^2 \phi_{\pm}}{dz^2} = -e(n_{i\pm} - n_{e\pm}), \quad (4)$$

where $n_{i\pm}$, $n_{0\pm}$, $u_{i\pm}$, u_B , ϕ_{\pm} , m_i , T_e , k , and λ_i denote ion density, electron density at $u_{i\pm} = u_B$, ion fluid velocity, Bohm velocity, electrostatic potential, ion mass, electron temperature, Boltzmann constant, and ion-mean-free path, respectively. z is the vertical coordinate from the cathode surface toward the bulk plasma, and the subscript +/- corresponds to (+)/(-) phase, respectively. In order to obtain the plasma structure at each (+) and (-) phase, Eqs. (1)–(4) were solved twice with the boundary conditions relevant to the two cases of $V_C = V_+$ and $V_C = V_-$. For the boundary conditions, the quasineutral limit ($n_{e\pm} = n_{i\pm}$) solution of Eqs. (1)–(4) was utilized. Since it is expressed as an analytic function of z , ϕ_{\pm} , $u_{i\pm}$, and $n_{i\pm}$ can be easily evaluated at sufficiently distant position from the sheath, i.e., at the bulk plasma where the quasineutral solution is valid.¹¹ It provided

good starting values for the fourth-order Runge–Kutta integration from the bulk plasma to the cathode. In addition, experimental values were used for other parameters such as T_e , $n_{0\pm}$, and λ_i obtained from the probe and pressure measurements. Consequently, the time-averaged values of the electron and ion densities, potential, and ion fluid velocity can be expressed as $\bar{n}_e = (n_{e+} + n_{e-})/2$, $\bar{n}_i = (n_{i+} + n_{i-})/2$, $\bar{\phi} = (\phi_+ + \phi_-)/2$, and $\bar{u}_i = (u_{i+} + u_{i-})/2$, respectively, aided by the square wave form assumption.

The particle charge was self-consistently evaluated from the plasma model. It is pointed out that the charging process has a finite relaxation time comparable to $1/f_{ac}$ since f_{ac} was given in experiment by a comparable value to the dust charging time. Therefore, the charge should be time averaged after the integration of the following charging equation described by instantaneous quantities of the electron and ion fluxes, in contrast to the evaluation of the other parameters such as electric field and ion density. To evaluate the dust charge, the orbital-limited motion theory of a spherical probe was applied with considerations of the ion thermal motion,^{14,15}

$$\frac{dQ(t)}{dt} = e\pi a^2 \left[n_i(t) v_{ii} \left\{ F_1\left(\frac{u_i(t)}{v_{ii}}\right) - F_2\left(\frac{u_i(t)}{v_{ii}}\right) \frac{Q(t)e}{4\pi\epsilon_0 a k T_i} \right\} - n_e(t) v_{ie} \exp\left(\frac{Q(t)e}{4\pi\epsilon_0 a k T_e}\right) \right], \quad (5)$$

where $Q(t)$ and a denote the dust charge and radius, and $v_{ii} = \sqrt{8kT_i/\pi m_i}$, $v_{ie} = \sqrt{8kT_e/\pi m_e}$, $F_1(x) = \sqrt{\pi}(1+2x^2) \text{erf}(x)/4x + \exp(-x^2)/2$, $F_2(x) = \sqrt{\pi} \text{erf}(x)/2x$, respectively. In Eq. (5), the instantaneous ion fluid velocity and electron/ion density are expressed as

$$u_i(t) = \begin{cases} u_{i+} & \text{if } l/f_{ac} \leq t < (l+1/2)/f_{ac} \\ u_{i-} & \text{if } (l+1/2)/f_{ac} \leq t < (l+1)/f_{ac} \end{cases}, \quad (6)$$

$$n_s(t) = \begin{cases} n_{s+} & \text{if } l/f_{ac} \leq t < (l+1/2)/f_{ac} \\ n_{s-} & \text{if } (l+1/2)/f_{ac} \leq t < (l+1)/f_{ac} \end{cases}, \quad (7)$$

where l is an integer and the subscript $s=e, i$. Equation (5) was solved by the fourth-order Runge–Kutta method until the charge converges to a periodic solution $Q(t)$, then it was averaged over one period $1/f_{ac}$ to obtain \bar{Q} .

For calculating various forces that the particles experience,¹⁰ only the aforementioned time-averaged quantities were used. The gravity and the friction coefficient η of the neutral drag force¹⁶ were directly evaluated from the size and mass density of the dust particle, gas pressure, and the gas temperature. The friction coefficient η was also measured in our experiment using the same method as in Ref. 17 by fitting small oscillation spectrum to Lorentzian, which resulted in the consistent value as the modeling. The electrostatic force $\bar{Q}\bar{E}$ and the ion drag force were evaluated by using the particle charge obtained from Eq. (5). The ion drag force was evaluated using the following formula:^{10,18,19}

$$F_{id} = \bar{n}_i m_i \sqrt{\pi} a^2 v_i^2 \int_0^\infty du \frac{e^{-(u^2+u_0^2)}}{u_0^2} \times [2u_0u \cosh(2u_0u) - \sinh(2u_0u)] \times \left[u^2 + 2\epsilon + 4 \frac{\epsilon^2}{u^2} \ln \frac{1 + \delta^{-2}(u^4 + 2\delta u^2)}{1 + \epsilon^{-2}(u^4 + 2\epsilon u^2)} \right], \quad (8)$$

where $u_0 = \bar{u}_i/v_i$, $v_i = \sqrt{2kT_i/m_i}$, $\epsilon = \bar{Q}e/4\pi\epsilon_0 m_i v_i^2 a$, $\delta \equiv \bar{Q}e/4\pi\epsilon_0 m_i v_i^2 \lambda_D$, λ_D is the screening (Debye) length of the plasma, and a is the particle radius, respectively.

B. Oscillation model

In many previous works where dust oscillations were induced by imposing an oscillating voltage to the excitation wire located near the cathode or rf electrode, the oscillating voltage application appeared to make little effect on plasma. As a result, it was considered that the applied voltage provided pure forced oscillations on a dust particle. However, since the excitation turned out to induce a nearly pure parametric oscillation under our experimental condition,¹⁰ we introduce a dust oscillation model in a similar approach as by Sorasio *et al.*⁷ in which nonlinear parametric oscillation is based on polynomial representation of the net trapping force in terms of position. Being different from the Sorasio's model where the displacement of the trapped particle was assumed to be sinusoidal in time, the observed vertical displacement $z_{\text{trap}}[V_{\text{exc}}(t)]$ induced by the excitation voltage was not sinusoidal in time in our experiment. In this study, therefore, we utilized the measured trap position at a given excitation voltage for evaluating the net force.

Assuming no flow and no temperature gradient of neutral gas, the equation of motion of a dust particle that is parametrically driven in the vertical direction perpendicular to the cathode can be expressed as

$$m_d \frac{d^2 z}{dt^2} = -\eta \frac{dz}{dt} + F_{\text{net}}\{z - z_{\text{trap}}[V_{\text{exc}}(t)]\}, \quad (9)$$

where the net force experienced by the particle is given by

$$F_{\text{net}}(z) = \bar{Q}\bar{E} + F_{id}(\bar{Q}, \bar{n}_i, \bar{u}_i) + m_d g,$$

and the sinusoidal voltage applied to the excitation wire is $V_{\text{exc}}(t) = V_0 \sin(2\pi f_{\text{exc}} t)$. $z_{\text{trap}}[V_{\text{exc}}(t)]$ indicates the trap position depending on the excitation voltage, m_d is the dust mass, and η is the friction coefficient of the neutral drag force. The time-averaged plasma parameters, potential $\bar{\phi}$, dust charge \bar{Q} , and various forces acting on the particle were calculated using the measured bulk plasma densities n_{0+} and n_{0-} , and the plasma model described in the preceding section.

IV. RESULTS AND DISCUSSIONS

Figure 3 represents the dependence of the measured vertical oscillation spectra of a 1.5 μm radius dust particle on

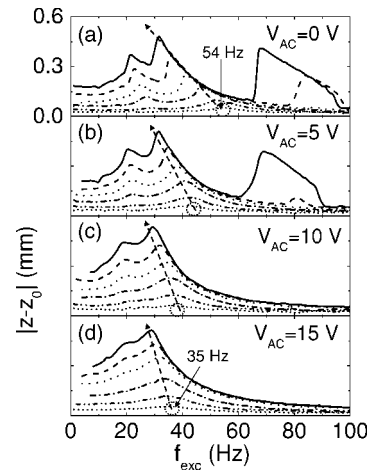


FIG. 3. Measured oscillation amplitude $|z-z_0|$ with different V_{ac} where z_0 is the particle equilibrium position. The applied f_{ac} was 1 kHz in all cases. Each set of the spectra was measured at six excitation voltages ($V_{\text{exc}}=0.8, 2, 4, 6, 8,$ and 10 V) by sweeping the excitation frequency (f_{exc}) from 1 Hz to 100 Hz with 0.5 Hz step. For the experimental conditions (without ac superposition) $a=1.5 \mu\text{m}$, $p=250$ mTorr, $V_C=-320$ V, $I_p=1$ mA, $n_p \approx 5 \times 10^9 \text{ cm}^{-3}$, $kT_e \approx 1$ eV. Dust particles were levitated at about 10 mm above the cathode surface.

the ac voltage superposed upon the dc cathode operated at 250 mTorr argon pressure. Each plot consists of oscillation spectra measured at six different excitation voltages ($V_{\text{exc}}=0.8, 2, 4, 6, 8,$ and 10 V), where the ordinate $|z-z_0|$ represents the oscillation amplitude with respect to the trap position z_0 . Figure 3(a) shows the measured spectrum without the ac superposition. Several observations can be made from the figure. First, for a small amplitude oscillation ($V_{\text{exc}}=1.0$ V), a Lorentzian spectrum of the linear forced oscillation having a single primary resonance peak at 54 Hz is seen. At larger V_{exc} , on the other hand, nonlinear features began to be observed. Above 2.0 V, a superharmonic resonance peak appeared at about half of the primary resonance frequency of which amplitude is largest. In addition, the resonance peak downshifted as V_{exc} was increased. At further larger V_{exc} over 8.0 V, a subharmonic resonance peak appeared at about twice of the primary frequency. The nonlinear features described above were commonly observed in oscillation spectra at low pressure plasmas where neutral drag is small.^{4,6-10} It is noted that the height of the subharmonic peak appeared to be comparable to that of the primary peak at the same V_{exc} , which is an evidence for the parametrically driven oscillations.⁸⁻¹⁰

Second, the most distinctive feature of the nonlinear oscillation characteristics is the dependence of the secondary resonance peaks on V_{ac} . As V_{ac} became larger, the subharmonic peak became smaller, which was not observed at all at further larger V_{ac} over 10 V. The superharmonic peak became also less prominent with increasing V_{ac} . It indicates that the ac modulation makes the dust oscillation less parametrically resonant. Third, by comparing the spectra of the small-amplitude oscillation ($V_{\text{exc}}=1.0$ V), it is seen that the primary resonance peak or the natural frequency downshifted from 54 Hz ($V_{ac}=0$ V) to 35 Hz ($V_{ac}=15$ V) as V_{ac} was increased. The downshift of the natural frequency indicates

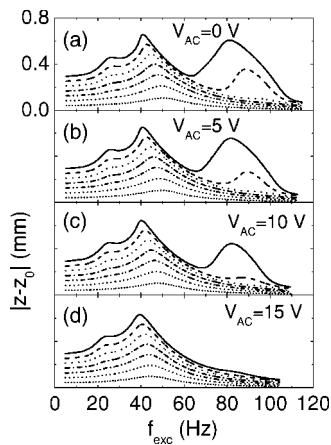


FIG. 4. Calculated frequency spectra vs V_{ac} at the same plasma and experimental conditions as those of Fig. 3. Each set of the spectra was presented in the same manner as Fig. 3 ($V_{exc}=1, 2, 3, 4, 5, 6,$ and 7 V).

that the force profile in the vicinity of the trap position was highly affected by the ac superposition. In addition, the slope of the dotted arrows in the figure shows that the amplitude-dependent (or V_{exc} dependent) shift of the resonance peak was also affected by the ac superposition. The resonance peak downshifted less with its amplitude as V_{ac} became larger.

All these the experimental results were consistent with the following numerical modeling results. Figure 4 shows four sets of frequency spectra versus V_{ac} that were calculated based on the same plasma density, electron temperature, gas pressure, particle size, and particle mass density measured in the experiment. Each set of the spectra was calculated with seven different excitation voltages ($V_{exc}=1, 2, 3, 4, 5, 6,$ and 7 V). As shown in the figure, the overall tendency was consistent with the experimental result (Fig. 3) except a little quantitative discrepancy. Figure 4(a) was calculated without ac superposition, which corresponds to the experimental result of Fig. 3(a). Comparison of Fig. 4(a) with Fig. 3(a) shows the overall oscillation characteristics agree with the measurement. While only one resonance peak (primary resonance) was found at low excitation voltages ($V_{exc} < 3$ V), the secondary resonance peaks (subharmonic and superharmonic peaks) appeared as V_{exc} was increased. The tendency of the downshift of the resonance peaks was also similar to that of the experimental result. Moreover, the subharmonic peak became smaller as V_{ac} became larger, and it finally vanished when $V_{ac} > 15$ V. From both experimental and theoretical results shown in Figs. 3 and 4 it is concluded that the ac modulation of the dc-biased cathode made the oscillatory motion of the trapped particle less nonlinear and less parametric. The results were also confirmed by Fig. 5, which presents the calculated charge and the net force profiles corresponding to the spectra shown in Fig. 4. The origin of the abscissa represents the particle trap or equilibrium position with $V_{ac}=0$. As shown in the charge profile in Fig. 5(a), the dust charge was reduced in its magnitude with V_{ac} in the vicinity of the trap position. The change of the charge profile was directly reflected in the force profile shown in Fig. 5(b). As V_{ac} was increased, the force profile became more linear and the slope

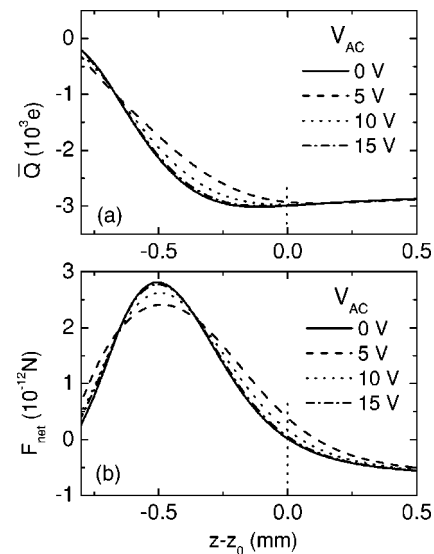


FIG. 5. Calculated charge and force profiles at five different V_{ac} .

at the trap position that is related to the primary resonance frequency at small-amplitude oscillations decreased. This observation agrees with the spectrum measurement discussed above. Consequently, it is found that the cathode ac modulation modified the oscillation spectra through the change of the dust charge profile and the force profile.

In the following, a detailed description is given on how the dust charge can be actively controlled by the ac modulation frequency f_{ac} even at the fixed V_{exc} . As shown in Fig. 6 where the oscillation spectra at several different f_{ac} at constant $V_{ac}=15$ V were given, the subharmonic peak decreased significantly as f_{ac} was lowered while other oscillation characteristics were pretty much unchanged. At lower f_{ac} than 1 kHz, the peak was not observed. The calculated spectra

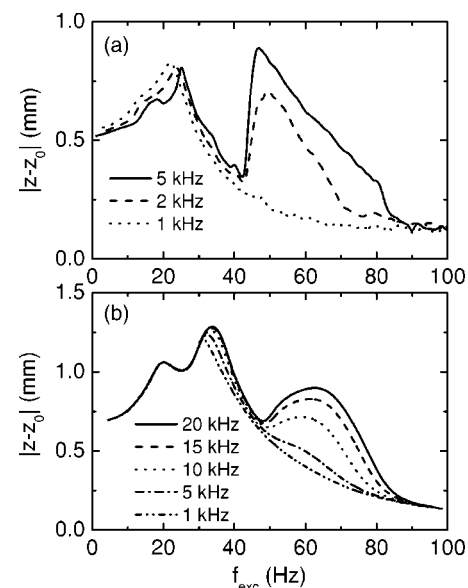


FIG. 6. (a) Measured oscillation spectra vs f_{exc} at $V_{ac}=15$ V and $V_{exc}=10$ V. The measurement was performed with $a=2$ μ m particles and other experimental conditions were same as those of Fig. 3. (b) Calculated spectra at the same conditions.

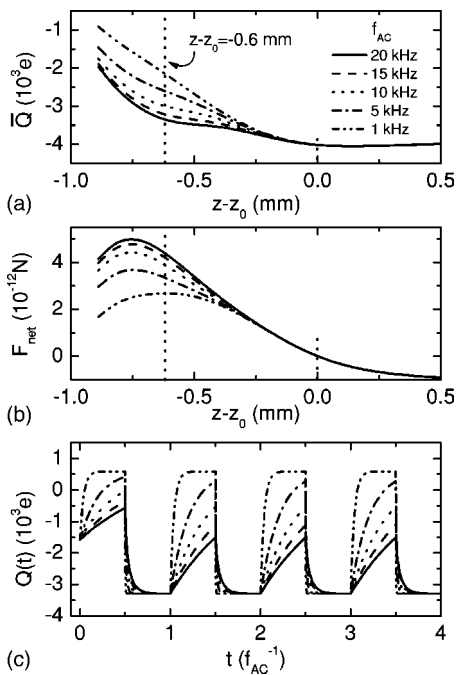


FIG. 7. (a) Charge and (b) force profiles at different f_{ac} , which correspond to Fig. 6. (c) Dependence of instantaneous dust charge at $z-z_0=-0.6$ mm on f_{ac} .

shown in Fig. 6(b) confirm the experimental observation. The dependence of the subharmonic resonance on f_{ac} is known to be strongly related to whether the oscillation was excited parametrically or by an external drive.^{7,9,10} Figures 7(a) and 7(b) show the charge and net force profiles corresponding to Fig. 6(b), which provides an insight about the oscillation driving scheme. The difference in the spectra was originated solely from the change of the charge profile because the calculation showed that the plasma structure such as plasma density and electric field did not vary with f_{ac} except the dust charge. In the charge profile, the magnitude of the charge below the trap position z_0 became smaller than that of the unmodulated case ($V_{ac}=0$). This tendency of the charge profile was directly reflected to the force profile in Fig. 7(b). As f_{ac} was decreased, the curvature of the force profile below the trap position ($z-z_0 < 0.5$ mm) was smoothened. Additionally, the natural frequency was found to be almost unchanged, which was directly shown in the net force slopes at $z-z_0=0$. From the comparison of Fig. 7 with Fig. 6, the suppression of the subharmonic resonance peak was found to be directly connected to the change of the force profile, which in turn was originated from the charge profile.

Figure 7(c) summarizes the relationship of the instantaneous dust charge $Q(t)$ with f_{ac} in terms of time expressed in periods. At low frequency (1 kHz), the charge evolution in the ion current rich phase (rising phase) was not very different from that in the electron current rich phase (falling phase). At high frequency (20 kHz), however, the rising time scale is much slower than the falling time scale because of the small ion mobility. As can be expected from the figure, the time average of the charge becomes smaller in magnitude as f_{ac} is decreased, which is already seen in Fig. 7(a). There-

fore, we can conclude that the charge profile is the main determinant of whether the trapped dust particles oscillate parametrically or not.

V. CONCLUSIONS

This work investigated the modification of the dust oscillatory behavior using ac voltage superposition on a dc cathode by separate control of the dust charge through both experimental and theoretical approaches. It was experimentally shown that the ac-superposed cathode was found to make the nonlinearity and the parametric resonance of the particle oscillation weak. The hysteresis did not occur, and the subharmonic resonance peak also disappeared as V_{ac} was increased. These changes in oscillation characteristics were confirmed by the charge and the force profile calculation. As a result, it is concluded that the cathode ac modulation made the dust oscillations less nonlinear and less parametrically resonant, which may suggest the controllability of the dynamic properties of the particles.

The dependence of the oscillation spectrum on f_{ac} was studied to demonstrate the separate control of the dust charge. As f_{ac} was decreased from 5 kHz to 1 kHz under the same V_{ac} , the subharmonic peak was significantly reduced with f_{ac} . This observation demonstrates that the dust charge profile mainly determines the property of the subharmonic peak, i.e., whether the oscillation is parametrically resonant or not. Consequently, we expect that modification of the dynamics of dust particles and, furthermore, independent charge control may be possible by the ac modulation of the dc biased cathode.

ACKNOWLEDGMENTS

This work was partly supported by the Vacuum Center at Korea Research Institute of Standards and Science, partly by the Korea Ministry of Science and Technology, and partly by the Korea Basic Science Institute.

- ¹G. S. Selwyn, J. Singh, and R. S. Bennett, *J. Vac. Sci. Technol. A* **7**, 2758 (1989).
- ²N. Sato, G. Uchida, T. Kaneko, S. Shimizu, and S. Iizuka, *Phys. Plasmas* **8**, 1786 (2001).
- ³N. Sato, G. Uchida, R. Ozaki, S. Iizuka, and T. Kamimura, in *Frontiers in Dusty Plasmas*, edited by Y. Nakamura, T. Yokota, and P. K. Shukla (Elsevier Science, Amsterdam, 2000), p. 329.
- ⁴A. V. Ivlev, R. Sutterlin, V. Steinberg, M. Zuzic, and G. Morfill, *Phys. Rev. Lett.* **85**, 4060 (2000).
- ⁵C. Zafiu, A. Melzer, and A. Piel, *Phys. Rev. E* **63**, 066403-1 (2001).
- ⁶Y. Wang, L. Hou, and X. Wang, *Phys. Rev. Lett.* **89**, 155001-1 (2002).
- ⁷G. Sorasio, D. P. Resendes, and P. K. Shukla, *Dusty Plasmas in the New Millennium*, edited by R. Bharuthram, M. A. Hellberg, P. K. Shukla, and F. Verheast, AIP Conf. Proc. (AIP, Melville, NY, 2002).
- ⁸G. Sorasio, D. P. Resendes, and P. K. Shukla, *Phys. Lett. A* **293**, 67 (2002).
- ⁹D. P. Resendes, G. Sorasio, and P. K. Shukla, *Phys. Plasmas* **9**, 2988 (2002).
- ¹⁰S. Park, C. R. Seon, and W. Choe, *Phys. Plasmas* **11**, 5095 (2004).
- ¹¹K.-U. Riemann, *Phys. Plasmas* **4**, 4158 (1997).
- ¹²K.-U. Riemann, *J. Phys. D* **36**, 2811 (2003).
- ¹³M. A. Lieberman and A. J. Lichtenberg, *Principles of Plasma Discharges and Materials Processing* (Wiley, New York, 1994), p. 170.
- ¹⁴M. S. Barnes, J. H. Keller, J. C. Forster, J. A. O'Neill, and D. K. Coultas, *Phys. Rev. Lett.* **68**, 313 (1992).

- ¹⁵P. K. Shukla, in *The Physics of Dusty Plasmas*, edited by P. K. Shukla, D. A. Mendis, and V. W. Chow (World Scientific, Singapore, 1999), p. 107.
- ¹⁶P. S. Epstein, *Phys. Rev.* **23**, 710 (1924).
- ¹⁷B. Liu, J. Goree, V. Nosenko, and L. Boufendi, *Phys. Plasmas* **10**, 9 (2003).
- ¹⁸J.-P. Boeuf and C. Punset, in *Dusty Plasmas: Physics, Chemistry, and Technological Impact in Plasma Processing*, edited by A. Bouchoule (Wiley, New York, 1999), p. 34.
- ¹⁹S. A. Khrapak, A. V. Ivlev, G. E. Morfill, and H. M. Thomas, *Phys. Rev. E* **66**, 046414-1 (2002).